

RSC Advances



This is an *Accepted Manuscript*, which has been through the Royal Society of Chemistry peer review process and has been accepted for publication.

Accepted Manuscripts are published online shortly after acceptance, before technical editing, formatting and proof reading. Using this free service, authors can make their results available to the community, in citable form, before we publish the edited article. This *Accepted Manuscript* will be replaced by the edited, formatted and paginated article as soon as this is available.

You can find more information about *Accepted Manuscripts* in the [Information for Authors](#).

Please note that technical editing may introduce minor changes to the text and/or graphics, which may alter content. The journal's standard [Terms & Conditions](#) and the [Ethical guidelines](#) still apply. In no event shall the Royal Society of Chemistry be held responsible for any errors or omissions in this *Accepted Manuscript* or any consequences arising from the use of any information it contains.

1 **Lithium iron phosphate (LiFePO₄) as an effective activator for**
2 **degradation of organic dyes in water in the presence of persulfate**

3 Xue-ming Lin^a, Yong-wen Ma^{a,b,c,*}, Yan Wang^{a,c}, Jin-quan Wan^{a,b,c}, Ze-yu Guan^a

4 **Abstract**

5 Lithium iron phosphate (LiFePO₄) was prepared and applied in heterogeneous
6 activation of persulfate (PS) for Orange G (OG) degradation in water. Scanning
7 electron microscopy, X-ray diffraction, Raman spectroscopy, X-ray photoelectron
8 (XPS) were used to characterize the properties of the material before and after
9 activation. The effect of several parameters on its catalytic activity was also
10 investigated. It was found that the catalyst presented ultrafast activity for OG and
11 other organic dyes degradation. Results from XPS further suggested that the highly
12 catalytic efficiency possibly involved the activation of PS to sulfate radicals as main
13 radical mediated by the redox pair of Fe(II)/Fe(III) of LiFePO₄/ FePO₄.

14 **Keyword:** LiFePO₄;Persulfate;Orange G; Degradation

15

16

^aCollege of Environment and Energy, South China University of Technology, Guangzhou 510006, China

^bState Key Laboratory of Pulp and Paper Engineering, South China University of Technology, Guangzhou 510640,
China

^cThe Key Laboratory of Pollution Control and Ecosystem Restoration in Industry Clusters, Ministry of Education,
South China University of Technology, Guangzhou 510006, China

1 1. Introduction

2 Efficient removal of organic pollutants from water is one of the major objective of
3 environment treatment. Advanced oxidation process based on sulfate radical is
4 recognized as an effective way for degradation of organic pollutant in the past decades.
5 The sulfate radical can be produced by activation of persulfate (PS) or
6 peroxymonosulfate (PMS) by UV, heat or catalyst and so on [1-3]. It should be
7 pointed out that the homogeneous Fenton-like process has significant disadvantages.
8 The homogeneous process needs high amounts of iron ions in the solution and the
9 produced iron ions need to be separated from the system at the end of the reaction,
10 which brings an additional removal process[4,5]. In recent years, the heterogeneous
11 activation of PS or PMS to produce sulfate radical to degrade pollutant has become a
12 more focused area. For example, Luo et al. prepared octahedral molecular sieve
13 (OMS-2) by a reflux method and investigated the performance of OMS-2/PMS
14 system using Acid Orange 7 (AO7) as a model compound [6]. Yuan et al. found that
15 ferrous sulfide ore particles presented very good and stable performance for the
16 degradation of p-chloroaniline with PS [7]. Li et al. reported degradation of methyl
17 orange by sodium persulfate activated with zero-valent zinc [8].

18 Now, in this paper, we herein report the use of LiFePO_4 crystals called LFP as an
19 efficient catalyst for the removal of organic pollutants using PS as an environmentally
20 beginning oxidant. LFP has been investigated intensively as a promising cathode
21 material due to its high energy density, low cost, chemical stability and safety [9-11].

1 However, to my best of our knowledge, this is the first try to use LiFePO_4 crystals as a
2 catalyst for the degradation of organic contaminants with PS as oxidant.

3 The aim of this study is to assess the catalytic performance and mechanism of
4 LiFePO_4 as heterogeneous persulfate activator on the Fenton-like oxidation of
5 different kinds of organic dyes among which Orange G (OG) was used as the main
6 model compound. This study is attempt to further advance the use of materials which
7 contain Fe as persulfate activator and broaden the range of application of materials
8 such as LFP.

9 **2. Materials and methods**

10 **2.1 Materials**

11 Unless otherwise indicated, all chemicals used in this study were reagent grade.
12 Ultrapure water was produced by a Millipore milli-Qsystem. The ammonium Fe (II)
13 sulfate hexahydrate and phosphoric acid were obtained from Sinopharm Chemical
14 Reagent Co., Ltd (Beijing, China). Lithium hydroxide and the dyes all were purchased
15 from Aladdin chemistry Co., Ltd (Shanghai, China) and used without any further
16 purification.

17 **2.2 Preparation of LiFePO_4**

18 LiFePO_4 crystals were synthesized by a solvothermal method similar to that
19 reported on the literature with certain modification. LiFePO_4 samples were made by
20 hydrothermal synthesis with an excess amount of Li to prevent Fe from occupying the

1 Li sites and blocking the Li diffusion channel [12-14]. Briefly, ammonium Fe (II)
2 sulfate hexahydrate (7.3525 g) and phosphoric acid (1.8375 g) were dissolved into 50
3 mL of water. Lithium hydroxide (2.3625 g) was also dissolved into 12.5 mL of water.
4 And then, these two solutions were quickly mixed under vigorous magnetic stirring at
5 room temperature. After stirring for 2 min, the mixture was poured into a 100-mL
6 Teflon-lined autoclave. The autoclave was heated in a furnace at 220°C for 2.5h. The
7 as-synthesized LFP could be easily separated by using a filter paper. After being
8 washed by ethanol for three times, the LFP particles were dried at 60°C
9 in a vacuum oven for 24 h.

10 **2.3 Characterization**

11 The morphology of LFP was observed by the thermal scanning electron
12 microscope (FESEM, Quanta 200, Holland). BET surface area of the prepared
13 catalyst LFP was measured using a surface area analyzer (ASAP 2020, micromeritics).
14 The crystallographic structures of the oxides were determined by an X-ray
15 diffractometer D8 Advance X-ray Diffraction system and Bruker AXS with a copper
16 target tube radiation (Cu K α 1) producing X-rays at a wavelength of 0.15418 nm.
17 Raman spectroscopy was recorded by the Raman spectrometer (LabRAM Aramis,
18 HORIBA JOBIN Yvon) comprising 0.1 M HClO $_4$ as electrolyte, a platinum wire
19 counter electrode, and an Ag/AgCl reference electrode. XPS was performed using an
20 X-ray Photoelectron Spectroscopy (ESCA) spectrometer (Thermo
21 SCIENTIFIC ESCALAB 250), with a monochromatized Al-K X-ray source, operated
22 at a power of 150 W.

1

2 **2.4 Catalytic degradation experiment and analysis**

3 Stock solutions of Orange G (OG) and persulfate were prepared by adding a
4 required amount of pure OG and persulfate. Since PS is an acidic oxidant, the addition
5 of PS led to a significant decrease of pH. And because the addition of PS alone can't
6 make contribution to organic pollutant removal (see Fig.3A), the initial pH was
7 adjusted to 2.9 with NaOH (0.1 M) and H₂SO₄ (0.1 M) solution after the addition of
8 PS. The flask was open to the atmosphere and shaken at 180 rpm in a rotary shaker
9 (ZHWY-20102C, Shanghai, China) at 25 ± 0.2°C. The degradation experiments of
10 other organic dyes, Acid Orange 7 (AO7), Rhodamine B (RhB), methylene blue (MB)
11 and methyl orange (MO) were similar to degradation experiment of OG. To monitor
12 the degradation process of organic dyes, solution samples were taken out at given
13 time intervals with solid removal and measured immediately. Residual dye was
14 analyzed by UV–Vis spectrophotometry method (Tianmei, UV2310-II) at a maximum
15 absorption wavelength. The maximum absorption wavelengths of OG, AO7, RhB,
16 MB and MO are 478, 487, 552, 664 and 463 respectively. Tests were run in triplicate
17 and the error bars were shown in figures to denote the standard deviation errors.

18 **3. Results and discussion**

19 **3.1 Characterization of LiFePO₄**

20 Fig.1A presents the morphology of prepared LiFePO₄ catalyst samples. As shown

1 in Fig.1A, rodlike morphology was depicted for the catalyst sample prepared. These
2 rods appeared similar form in size. The average length of LFP rods was between
3 about 150 and 300 nm, which was much shorter in length and smaller in morphology
4 compared to what the literature showed [12]. The measurement of Brunauer–Emmet–
5 Teller (BET) surface showed that the synthesized catalyst had a BET surface area of
6 about $36.2\text{m}^2/\text{g}$, which was much larger than the literatures showed because the size
7 of the catalyst became smaller than the literature showed. The larger BET could lead
8 to more active sites for the activation of PS, which was conducive to the removal of
9 the pollutants.

10 The X-ray diffraction patterns of LiFePO_4 catalysts prepared by a solvothermal
11 method were shown in Fig.2 (A). All peaks can be indexed to triphylite phase (JCPDS
12 040-1499, Triphylite). By using the Scherrer equation for the (111) peak and (131)
13 peak from XRD data, the value was calculated to be about 29 nm [13].

14 The Raman experiments of initial LFP were shown in Fig.2 (B). Because of the
15 small particle size, not all the external and internal modes of LiFePO_4 previously
16 reported were observed in the initial materials. In addition, because of the impurities
17 such as Li_3PO_4 , Fe_3O_4 , FePO_4 and so on [15], the peaks did not absolutely belong to
18 LiFePO_4 . Still, the most intense symmetric stretching peak at 1001 can be clearly
19 identified as non-distorted PO_4^{3-} tetrahedral in the pristine LiFePO_4 . Besides, the
20 bands at $200\text{--}400\text{ cm}^{-1}$ correspond to the Raman vibrations of Fe–O in LiFePO_4
21 [16,17].

1 **3.2 Catalytic activity of LFP**

2 The catalytic performance of different combination was shown in Fig.3 (A). From
3 Fig.3 (A) it can be seen that LFP/PS system showed high efficiency for OG
4 degradation with a removal of 93.6% after 10 min, while the addition of PS or LFP
5 alone brought negligible removal of OG even after 20min. In addition, the activity of
6 the LFP/PS system for degradation of other dyes such as AO7, RhB, MO and MB was
7 also examined under similar conditions. As shown in Fig.3 (B), all the dye pollutants
8 could also be decolorized efficiently. These results clearly indicated that the LFP/PS
9 system was an efficient system for decolorization of dyes wastewater.

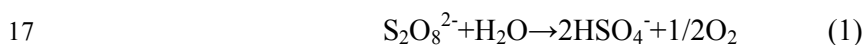
10 **3.3 Effect of reaction parameters on activity of LFP/PS system**

11 In order to know the activity of LFP/PS system in practical application, PS
12 concentration, LFP dose, and pH as main factors on the catalytic behavior of LFP/PS
13 system were studied.

14 In what concerns the treatment process efficiency and operational costs, PS has a
15 high impact. To elucidate the role of PS concentration on the degradation of OG,
16 some experiments were carried out by varying the initial PS concentrations. As shown
17 in Fig.4, the decolorization rate became higher and higher when the PS concentration
18 increased. More persulfate concentration led to more contact opportunities for LFP
19 and PS, accordingly more $\text{SO}_4^{\cdot -}$ were generated from the homogeneous and
20 heterogeneous reaction .

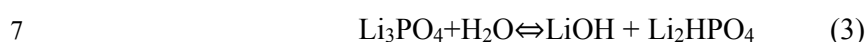
21 Fig.5 illustrates the OG decolorization by PS/LFP system at various amount of

1 LFP. The results demonstrated that when the amount of LFP was less than 0.5g/L and
2 pH was lower than 3, the degradation rate became higher and higher as the amount of
3 LFP increased. The fact was mainly attributed to the increased concentration of active
4 sites for reaction with PS. However, the results had little change between 0.5g/L and
5 0.6g/L. Perhaps the diffusion of OG and PS became the rate-limiting step under these
6 conditions. Fig.6 (A) presents the OG decolorization by PS/LFP system at various pH.
7 The results demonstrated that the degradation rate didn't change much when the pH
8 was low than 3. When the initial pH was more than 3, the degradation rate decreased
9 rapidly. The reason was that the increased pH after reaction (pH could increase much
10 easily when initial pH was higher than 3.5 or initial amount of LFP increased too
11 much, for example, to 1g/L) was bad for the activation of PS like what the literatures
12 showed [6,7]. As Fig.6 (B) shows, when the initial pH was lower than 3.0, the pH
13 changed little along the degradation experiment. However, when the initial pH
14 reached 5.0, pH increased quickly to 8.8 just in 2 mins. The pH declined a little after 6
15 min because of the decomposition of PS to produced additional H⁺ as the reaction (1)
16 and (2) show [18]:



19 To find the origin of the alkaline behavior of the LiFePO₄ sample, filtrate
20 solutions after pH measurements were collected and analyzed by ion chromatography
21 (IC) and Atomic Absorption Spectroscopy (AAS) which would be shown in Fig.9.

1 Compared Fig.6 (B) with Fig.9, we can know that the pH value of the filtrate
2 increased as the concentration of PO_4^{3-} ions and Li ions increased. And the molar ratio
3 of Li to PO_4^{3-} in the filtrate was close to 3 from the result of AAS and IC
4 measurement. These results strongly suggest that it was the dissociation of impurity
5 Li_3PO_4 in water that led to the high pH [15] , with a mechanism as equation (3)
6 showed.



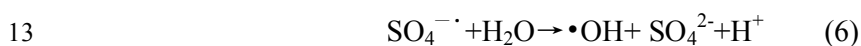
$$8 \quad \text{pH}_2 = -\lg(10^{-\text{pH}_1} - C_{\text{OH}}) \quad (4)$$

9 The relation of produced OH^- and H^+ can be approximately described by equation
10 (4). In equation (4), pH_1 , pH_2 and C_{OH} represented the initial pH, final pH and
11 concentration of produced OH^- respectively, and 10^{-pH_1} represented the initial
12 concentration of H^+ . As the equations showed, we could know that when the initial pH
13 was low enough, the produced OH^- could be too low to increase the solution pH
14 compared to the high H^+ concentration (lower pH is related to higher H^+ concentration
15 because H^+ concentration is equal to $10^{-\text{pH}}$). Thereby, when initial pH was less than 3,
16 the pH of process would keep around 3 and the decolorization rate would keep high as
17 Fig 6 showed. This can also explained why high pH (maybe just more than 3.5) would
18 decrease the reaction rate rapidly.

19 **3.4 Identification of predominate radical species**

20 Radical inhibition experiments were conducted to identify the dominant radical

1 oxidant ($\text{SO}_4^{\cdot-}$ vs. $\cdot\text{OH}$) by observing the differences in radical reactivity toward two
2 different alcohol additives, ethanol containing alpha hydrogen and TBA with no alpha
3 hydrogen. The reaction of $\text{SO}_4^{\cdot-}$ with TBA ($4\text{--}9.1\cdot 10^5\text{M}^{-1}\text{s}^{-1}$) is reported to be
4 considerably slower than that with a secondary or primary alcohol (e.g., EtOH, 1.6--
5 $7.7\cdot 10^8\text{M}^{-1}\text{s}^{-1}$). However, the $\cdot\text{OH}$ reacts rapidly with not only EtOH containing
6 a-hydrogen at a rate of $1.2\text{--}2.8\cdot 10^9\text{M}^{-1}\text{s}^{-1}$ but also TBA containing no a-hydrogen at a
7 rate of $3.8\text{--}7.6\cdot 10^8\text{M}^{-1}\text{s}^{-1}$ [19]. Therefore, ethanol is an effective quencher for both
8 $\text{SO}_4^{\cdot-}$ and $\cdot\text{OH}$, while TBA is an effective quencher for $\cdot\text{OH}$ but not for $\text{SO}_4^{\cdot-}$. The
9 production of $\text{SO}_4^{\cdot-}$ and $\cdot\text{OH}$ can be explained by the possible reaction equation (5)
10 and (6). The reaction mechanism shown below would be proven further in another
11 part of this article.



14 Fig.7 shows the rate of OG degradation in the presence of various quenching
15 reagents. When OG:PS:TBA=1:10:100, the catalytic activity was slightly inhibited,
16 and more addition of the TBA (OG:PS:TBA =1:10:1000) only decreased the rate a
17 little more. However, when OG:PS:EtOH =1:10:100, the decolorization rate was
18 largely decreased to only 54%. More addition of the EtOH (OG:PS:EtOH =1:10:1000)
19 made the decolorization rate less than 20%. This result suggested that the dominant
20 radical formed in the process was $\text{SO}_4^{\cdot-}$. Hydroxy radicals might be also present, but
21 its contribution was very little compared with sulfate radicals.

1 **3.5 Reusability and stability of the catalyst**

2 For a practical implementation of a heterogeneous catalytic system, it is crucial to
3 evaluate the stability of the catalysts. The activator was collected by filtration after
4 reaction, and the decolorization reaction was re-initiated by adding a fresh solution of
5 OG and PS. As shown in Fig.8, the efficiency decreased slowly as the number of
6 recycle increased, probably due to the activity of the catalyst decreased. As Fig.9
7 shows, during the reaction for 30mins, the Fe concentration in the reaction solution
8 was found less than 0.02mM by using AAS spectroscopy. Then another experiment
9 was established to check the role of the dissolved Fe ions for the observed catalytic
10 activity. FeSO₄·7H₂O (6mg/L) whose mole concentration was similar to the total
11 leached Fe of LFP was used instead of leached Fe to activate PS. However, the
12 degradation rate was low enough to be neglected. This could also prove that the
13 heterogeneous activation made primary contribution to the degradation of organic
14 pollutant. Compared to mole concentration of Fe, the mole concentration of PO₄³⁻ and
15 Li was about 0.26Mm and 1.45Mm respectively. The main reason of the large amount
16 of PO₄³⁻ and Li leached in the solution could be explained by the reaction equation (3).
17 The difference between the theoretical mole ratio of PO₄³⁻ and Li shown from
18 equation (3) and the actual ratio could be explained by equation (5). Because FePO₄
19 can't be dissolved in water, so the mole concentration of leached Fe was little to be
20 ignored.

21 The separated LFP activator after the third reaction run was further examined by

1 SEM, XRD and Raman with the results shown in Fig.1 and Fig.2. Compared to the
2 images of the fresh activator, the LFP rods were broken to little particles with average
3 diameter of about 30 to 100 nm. The XRD image of the recycled catalyst LFP showed
4 obscure peaks, which may indicate that the structures had some changes along the
5 catalyst experiment. In addition, the Raman image of used LFP had some new peaks
6 below 200cm^{-1} compared to fresh LFP, which represented the appearance of FePO_4
7 phase. The analysis of XRD and Raman together indicated that most structure of the
8 catalyst had changed to amorphous FePO_4 phase, which made the activity of the
9 catalyst decrease.

10 **3.6 Activation mechanism of PS on LFP**

11 From the analysis of section 3.4, we know that LFP could activate PS to produce
12 $\text{SO}_4^{\cdot-}$ and $\cdot\text{OH}$, and $\text{SO}_4^{\cdot-}$ was the predominant radical species. Though $\cdot\text{OH}$ could
13 be also generated by reaction of $\text{SO}_4^{\cdot-}$ with H_2O , the analysis presented that $\cdot\text{OH}$
14 made little contribution to the degradation of organic pollutants. After the analysis of
15 3.5, the catalyst mechanism shown in equation (5) was proven further. For further
16 analysis of the catalyst mechanism, X-ray photoelectron spectroscopy was applied to
17 analyze the catalyst before and after the reaction. X-ray photoelectron spectroscopy is
18 a surface characterization technique that provides qualitative and quantitative
19 information from the outermost few atomic layers [20]. It is extremely sensitive to
20 Fe^{2+} and Fe^{3+} and is often applied to study the compositions of mixed-valence iron
21 species [21]. The XPS survey spectrum of the LiFePO_4 obtained before and after

1 reaction were depicted in Fig.10 (A). The most significant features in these two
2 spectrums were Fe2p, O1s, and P2p signals. Therefore, the fitting results of XPS
3 spectrums of Fe2p, O1s, and P2p with Shirley method of background subtraction
4 [21,22] were shown in Fig. 10(B) (C) (D).

5 Fe2p spectrum was composed of a doublet structure due to multiples splitting (i.e.,
6 Fe2p_{3/2} and Fe2p_{1/2}) as shown in Fig. 10(B). Although it was possible to obtain
7 much better curve fitting when additional peaks were used, the difficulty in
8 identifying these peaks due to peak position proximity was the main reason behind
9 not using additional peaks. The Fe2p peak could be fitted well by a Gaussian–
10 Lorentzian product function after Shirley type background subtraction. For Fe2p_{3/2},
11 two peaks at 712.9 and 710.5 eV were obtained in the fresh LFP catalyst, which were
12 assigned to Fe(III) and Fe (II) oxidation states, respectively[23]. Their atom ratio was
13 42.2:57.8. After reactions, the two Fe species were still present in the catalyst, but
14 their atom ratio was changed to 52.3:47.7, indicating that Fe (II) on surface of the
15 used catalyst was transformed partially to Fe (III). From Fe 2p_{1/2} shown in the figure,
16 similar conclusions could be obtained.

17 As Fig.10 (C) showed, the O 1s peak before and after reaction could be
18 decomposed into 3 sub-component, and the main one (corresponding to 90% of the
19 total oxygen content) centered at 531.2 eV, in good agreement with values reported
20 for oxygen in lattice oxygen of PO₄³⁻. The two minor components were likely related
21 to surface contaminations. P 2p spectrum of fresh and used catalyst showed the

1 typical shape due to spin-orbit splitting. The position of the P 2p_{3/2} component at
2 133.2 eV, together with the position of the main O 1s component, indicated the
3 presence of the PO₄³⁻ group in the sample [24]. Combined with the analyses, it could
4 be indicated that parts of the used catalyst became FePO₄. It could be drawn a
5 conclusion that the activation mechanism of PS by LFP was as the equation (5)
6 showed.

7 **4. Conclusion**

8 The degradation of OG in aqueous solutions by LiFePO₄ in the presence of
9 persulfate had been studied. Nearly complete removal of OG and other organic dyes
10 could be achieved within 10 mins by PS/ LiFePO₄ system. To increase the PS
11 concentration and LFP amount properly would promote the dyes degradation when
12 pH was less than 3. With the increase of solution pH (especially more than 3), the
13 efficiency decreased rapidly. The quenching studies indicated that sulfate radicals
14 were the primary radicals species compared to hydroxyl radicals produced during the
15 activation of PS. Further study of XPS suggested that the highly catalytic efficiency
16 possibly involved the activation of PS to sulfate radicals as main radical mediated by
17 the redox pair of Fe(II)/Fe(III) of LiFePO₄/ FePO₄. As an environmental oxidation
18 process, the activation of PS by LiFePO₄ may have potential application in water
19 pollution treatment.

20 **Acknowledgements**

21 This study was funded by National Natural Science Foundation of China (No.

1 31570568), High-level Personnel Foundation of Guangdong Higher Education
2 Institutions (2013), State key laboratory of Pulp and Paper Engineering in China (No.
3 201535). The authors are thankful to all the anonymous reviewers for their insightful
4 comments and suggestions.

5

6

7

8 **References**

9 [1] S.Y. Yang, P. Wang, X. Yang, et al., *J. Hazard. Mater.*, 2010, 179, 1-3, 552-558.

10 [2] K.C. Huang, R.A. Couttenye, G.E. Hoag, *Chemosphere*, 2002, 49, 4, 413-420.

11 [3] R. Waldemer, P. Tratnyek, R. Johnson, et al., *Environ. Sci. Technol.*, 2007, 41,
12 1010-1015.

13 [4] M.M.Cheng, W.H.Ma., J.Li, Y.P.Huang, J.C.Zhao, *Environ.Sci.Technol.*, 2004, 38,
14 1569-1575.

15 [5] R.M.Liu, S.H. Chen, M.Y. Hung, C.S. Hsu, J.Y. Lai, *Chemosphere*, 2005, 59, 117
16 -125.

17 [6] S.L.Luo, D.N.Lian, B.Z.Sun, M.Y.Weii, X.X.Li. *Applied Catalysis B:*
18 *Environmental*, 2015, 164, 92-99.

- 1 [7] I.Hussain, Y.Q. Zhang, S.B. Huang, X.Z. Du., Chem. Eng.J., 2012, 203, 269–276.
- 2 [8] H.Li, J.Guo, L.J.Yang, Y.Q.Lan, Separation and Purification Technology, 2014,
3 132, 168–173.
- 4 [9] C. M. Julien, A. Mauge, A. Ait-Salah, M. Massot, F. Gendron, K. Zaghbi., Ionics,
5 2007, 13, 395–411.
- 6 [10]M.J. Li, L.Q.Sun, K.Sun, S.H.Yu, R.S.Wang, H.M. Xie. J.Solid State
7 Electrochem, 2012, 16, 3581–3586.
- 8 [11]J.F.Qian, M.Zhou, Y.L.Cao, X.P.Ai and H.X.Yang. J. Phys. Chem. C, 2010, 114,
9 3477–3482.
- 10 [12]Z.J.Li, G,Ali, H.J.Kim, S. H.Yoo and S.O.Cho, Nanoscale Research Letters, 2014,
11 9, 276.
- 12 [13]C.Y.Chiang, H.C.Su, P.J.Wu, H.J.Liu, C.W.Hu, N.Sharma and V. K. Peterson, J.
13 Phys. Chem. C, 2012, 116, 24424–24429.
- 14 [14]B.Ellis, W.H Kan, W.R.M Makahnouk, L.F.Nazar, J.Mater.Chem, 2007, 17,
15 3248–3254.
- 16 [15]Denis Y., W. Yu, K.Donoue, T.Kadohata, T.Murata, S.Matsuta and S.Fujitani,
17 J.Electrochem.Society, 2008,155, 7, A526-A530.
- 18 [16]J.Wu, G.K.P.Dathar, C.W Sun, et.al. Nanotechnology, 2013, 24.

- 1 [17]Z.M. Zheng, W.K.Pang, X.C.Tang, D.Z.Jia, Y.D.Huang and Z.P. Guo, Journal of
2 Alloys and Compounds, 2015, 640, 95–100.
- 3 [18]C.Hu, J C.Yu., H.Z, P.K.Wong, Appl.Catal. B: Environ., 2003, 46, 1, 35-47.
- 4 [19]C. Liang, H.W. Su. Ind. Eng. Chem. Res., 2009, 8, 5558–5562.
- 5 [20]J.A. Mielczarski, G.M. Atenas, E. Mielczarski. Appl. Catal. B: Environ., 2005, 56,
6 289–303.
- 7 [21]H.X. Li, J.Q. Wan, Y.W.Ma, M.Z.Huang, Y.Wang, Y.M.Chen., Chem.Eng. J.2014,
8 250, 137–147.
- 9 [22]K. Volgmann, F. Voigts, W. Maus-Friedrichs., Surf. Sci., 2012, 606,858–864.
- 10 [23]L. Castro,R. Dedryv`ere, J. B. Ledeuil,J. Br`eger,C. Tessier, D. Gonbeau,
11 J.Electrochem.Society, 2012, 159, 4, A357-A363.
- 12 [24]A.Paoella, G.Bertoni, P.Hovington, et.al., Nano Energy, 2015,16, 256–267.

Fig. 1. SEM spectra of (A) fresh and (B) used LFP catalyst

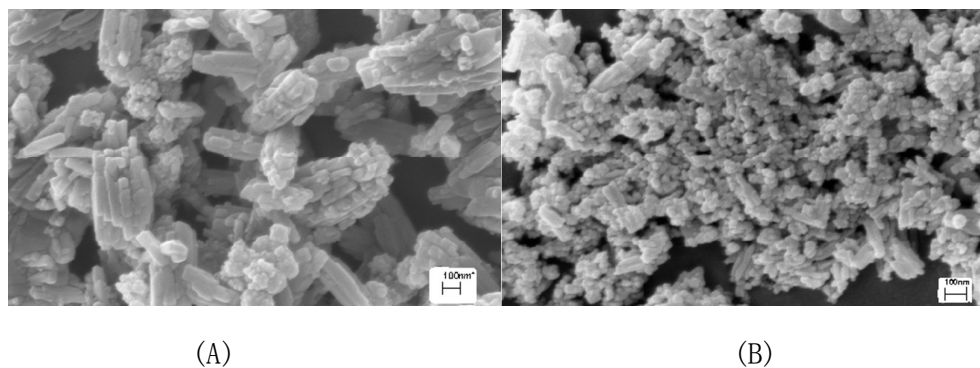


Fig. 2. (A) XRD and (B) Raman spectra of fresh and used LFP catalyst.

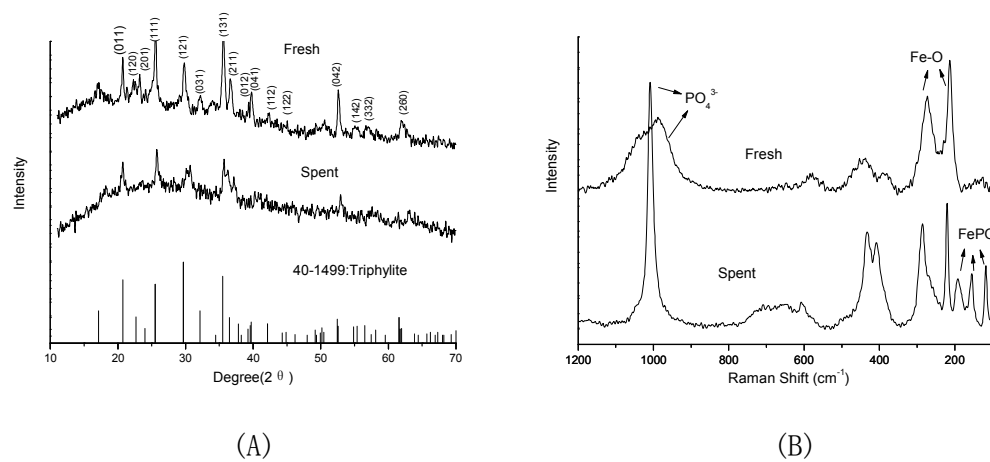


Fig.3 (A) OG Degradation with different systems and (B) degradation of other organic dyes with LFP/PS system. Conditions: LFP 0.2g/L, Fe_3O_4 0.2g/L, PS 2mM, Dyes 0.2mM, 25°C

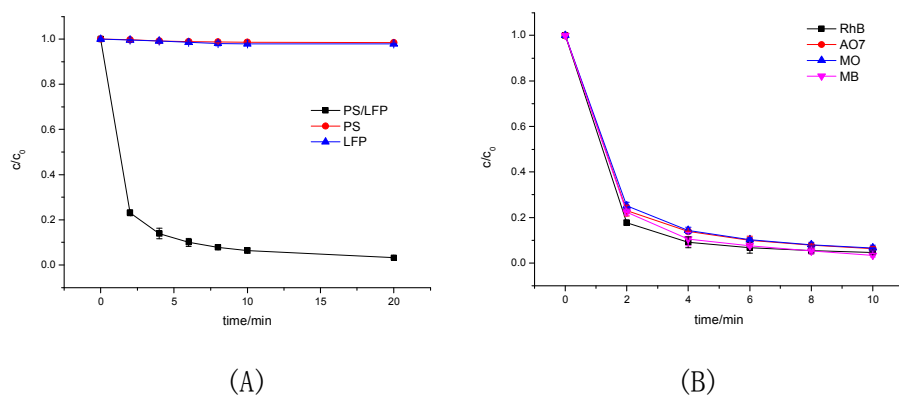


Fig.4. OG degradation with different PS concentration. Degradation condition: OG 0.2mM, LFP 0.2g/L, pH 2.90, 25°C

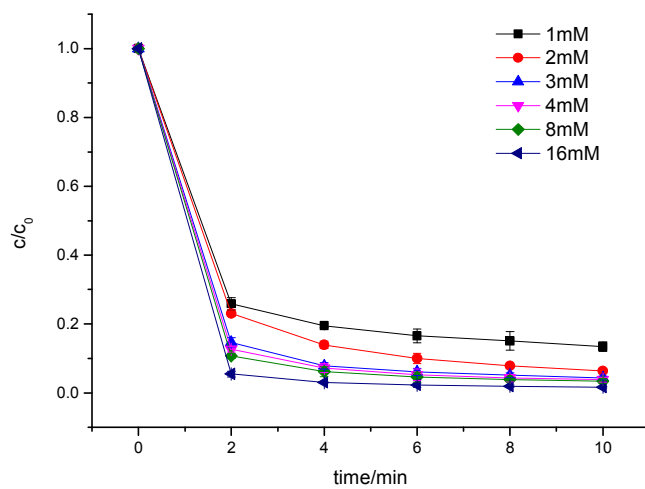


Fig.5. OG degradation with different amount of LFP. Experiment condition: OG 0.2 mM, PS 2Mm, pH 2.9, 25 °C, LFP (1)0.1g/L, (2)0.2g/L, (3)0.3g/L, (4)0.4g/L, (5)0.5g/L, (6)0.6g/L

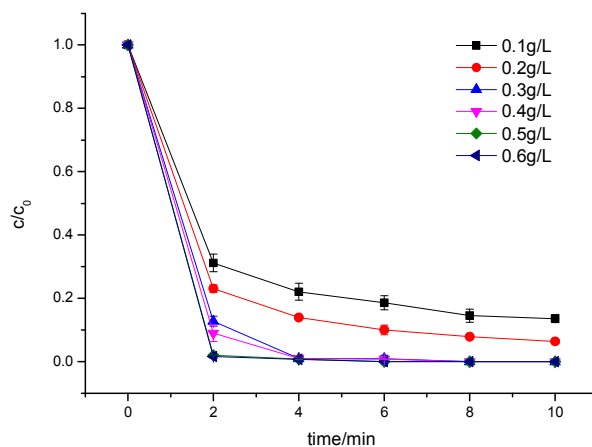


Fig.6. (A) OG degradation with different pH and (B) change of pH with different initial pH along time. Experiment condition: OG 0.2mM, PS2mM, LFP 0.2g/L, 25 °C

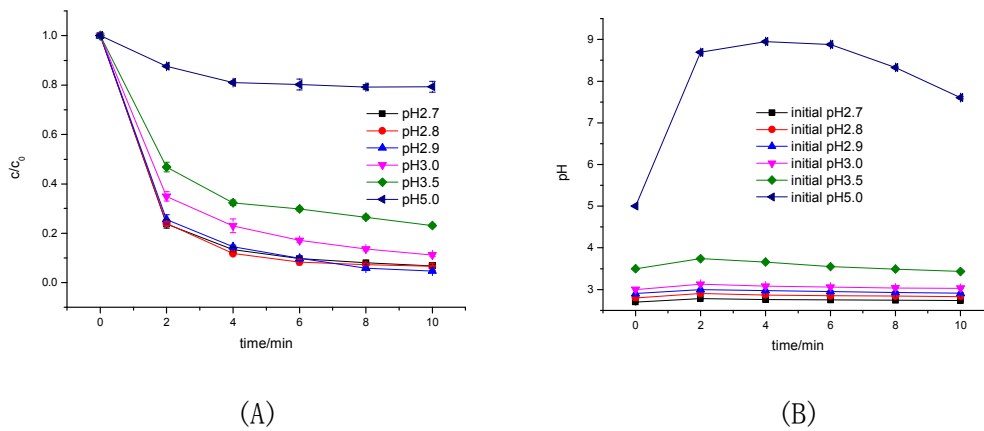


Fig.7. Inhibiting effect of EtOH and TBA on OG degradation with LFP/PS System.

Degradation condition: LFP 0.2g/L, PS 2mM, OG 0.2 mM, pH 2.9, 25°C

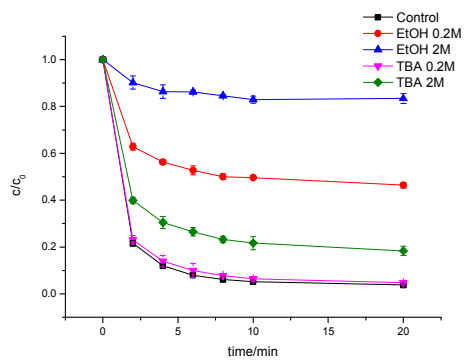


Fig.8 OG degradation in multi-cycle batch experiments. Condition: LFP 0.2g/L, OG

0.2mM, PS 2mM, initial pH 2.9, 25°C

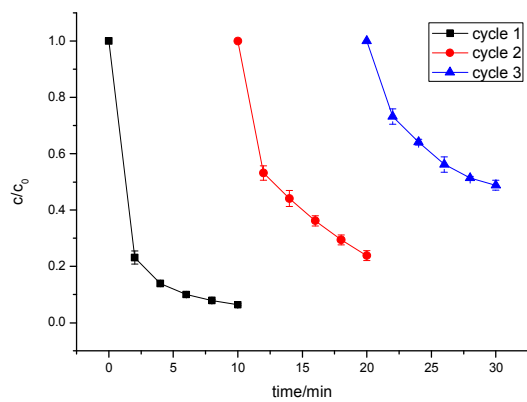


Fig. 9 The variation of dissolve Fe, Li, PO_4^{3-} and pH during the reaction. Condition: LFP 0.2g/L, OG 0.2mM, PS 2mM, initial pH 2.9, 25°C

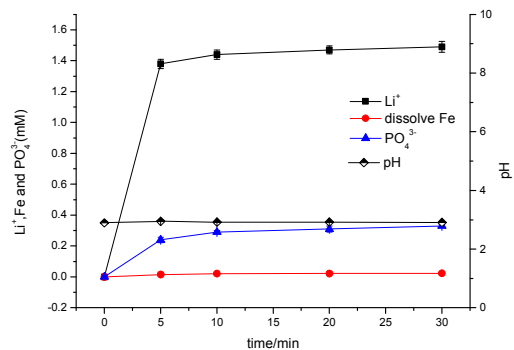


Fig.10 XPS of LFP before and after reaction. (A) Survey spectrum (B) Fe2p spectrum (C) O1s spectrum (D) P2p spectrum

